Hemodynamic effects of glutathione-liganded binuclear dinitrosyl iron complex: evidence for nitroxyl generation and modulation by plasma albumin

Taiming Liu, Meijuan Zhang, Michael H. Terry, Hobe Schroeder, Sean Wilson, Gordon Power, Qian Li, Trent E. Tipple, Dan Borchardt, Arlin Blood

Division of Neonatology, Department of Pediatrics, Loma Linda University School of Medicine, Loma Linda, CA 92354   TML, MJZ, AB.

Department of Respiratory Care, Loma Linda University School of Medicine, Loma Linda, CA 92354   MHT

Center for Perinatal Biology, Loma Linda University School of Medicine, Loma Linda, CA 92354   HS, SW, GP, AB

Neonatal Redox Biology Laboratory, Division of Neonatology, University of Alabama at Birmingham, Birmingham, AL 35294   QL, TET

Department of Chemistry, University of California, Riverside, CA, 92521   DB

Running title: Albumin modulates vasoactivity of HNO donor BDNIC

Address Correspondence to:

Arlin B. Blood

11175 Campus Street, 11121 Coleman

Loma Linda, CA 92354

Phone: 909-558-7448

Fax: 909-558-0298

Email: ablood@llu.edu

Number of text pages: 38

Word count (excluding references and figure legends): 5705

Tables: 0

Figures (all grayscale): 7

Reference numbers: 42

Supplementary Figures: 8

Word count (Abstract): 233

Word count (Introduction): 596

Word count (Discussion): 1788

List of abbreviations:

AS: Angeli's salt

BDNIC: binuclear DNIC

CPTIO: 2-(4-carboxyphenyl)- 4,4,5-tetramethyl imidazoline-1-oxyl-3-oxide

DNIC: dinitrosyl iron complexes

DTPA: diethylene triamine pentaacetic acid

DTT: 1,4-dithiothreitol

EDTA: ethylene diamine tetraacetic acid

glut-BDNIC: Glutathione-liganded binuclear dinitrosyl iron complex

GSH: glutathione

GSNO: S-nitroso-glutathione

HNO: nitroxyl

HMW: high molecular weight

HR: heart rate

LMW: low molecular weight

MAP: mean arterial blood pressure

MDNIC: mononuclear DNIC

NO: nitric oxide

NO^+: nitrosonium

NO·: free radical NO

NOS: NO synthase

ODQ: 1H-[1,2,4] oxadiazolo [4,3-a] quinoxaline-1-one

PIH: pyridoxal isonicotinoyl hydrazone

sGC: soluble guanylate cyclase

SOD: superoxide dismutase 1

Abstract: Glutathione-liganded binuclear dinitrosyl iron complex (glut-BDNIC) has been proposed to be a donor of nitric oxide (NO). This study was undertaken to investigate the mechanisms of vasoactivity, systemic hemodynamic effects, and pharmacokinetics of glut-BDNIC. To test the hypothesis that glut-BDNICs vasodilate by releasing NO in its reduced (HNO) state, a bioassay method of isolated, preconstricted ovine mesenteric arterial rings was used in the presence of selective scavengers of HNO or NO free radical (NO·), the vasodilatory effects of glut-BDNIC were found to have characteristics similar to those of an HNO donor and markedly different than a NO· donor. In addition, products of the reaction of glut-BDNIC with CPTIO (2-(4-carboxyphenyl)- 4,4,5-tetramethyl imidazoline-1-oxyl-3-oxide) were found to have electron paramagnetic characteristics similar to those of an HNO donor compared to an NO· donor. In contrast to S-nitroso-glutathione (GSNO), which was vasodilative both in vitro and in vivo, the potency of glut-BDNIC-mediated vasodilation was markedly diminished in both rats and sheep. Wire myography showed that plasma albumin contributed to this loss of hypotensive effects, an effect abolished by modification of the cysteine-thiol residue of albumin. High doses of glut-BDNIC caused long-lasting hypotension in rats that can be at least partially attributed to its long circulating half-life of ~44 min. This study suggests that glut-BDNIC is an HNO donor and that its vasoactive effects are modulated by binding to the cysteine residue of plasma proteins, such as albumin.

Introduction

Nitric oxide (NO) plays an important vasodilatory role in mammals including humans. NO synthase (NOS) enzymes are the primary source of NO in the body, but its bioactivity is more complex than simple diffusion of NO from NOS to its site of action. Instead, evidence suggests roles for a number of NO congeners that are capable of both preserving and regulating its bioactivity. Many derivatives of NO, such as dinitrosyl iron complexes (DNIC) (Mulsch et al., 1991; Rahmanto et al., 2012; Vanin, 2016), S-nitrosothiols (SNOs) (Pawloski et al., 2001) and nitrite (Cosby et al., 2003), have been proposed to stabilize, store, and transport NO bioactivity. Research on DNICs is limited in comparison to extensive studies on SNOs and nitrite, despite recent evidence that DNICs are the most prevalent intracellular NO adduct (Hickok et al., 2011).

Dinitrosyl iron complexes consist of an $Fe(NO)_2$ nucleus attached to anionic ligands. These ligands are often thiols and can range in size from small molecules such as L-cysteine and glutathione to high molecular weight proteins with thiol groups, such as albumin (Vanin, 2009). DNICs can exist with either one or two $Fe(NO)_2$ nuclei, termed mononuclear (MDNIC) and binuclear (BDNIC) DNICs, respectively (Supplemental Figure 1A) (Borodulin et al., 2014).

When applied to isolated arteries, low molecular weight M- and BDNICs synthesized with glutathione or L-cysteine ligands demonstrate vasodilatory potencies comparable to that of NO itself (Blum-Johnston et al., 2016; Vanin et al., 2007; Vanin et al., 1996). Although DNIC is capable of activating isolated soluble guanylate cyclase (sGC) (Severina et al., 2003), the

mechanism by which these compounds deliver NO moiety across the plasma membrane is not known. Even the redox state of the NO moiety in DNICs is uncertain. There are three different redox states of NO: nitrosonium (NO^+), free radical NO (NO·), and nitroxyl (HNO), each with similar but also distinctive biochemical properties (Flores-Santana et al., 2011; Shoman and Aly, 2016; Stamler et al., 1992). X-ray crystallography studies indicate the NO moieties of DNICs are partially negatively charged (Tsai et al., 2015), suggesting they may release HNO. However, others propose that DNICs exist with a partial positive charge on the NO moiety, in which case the DNICs would be more likely to release NO· or even NO^+ that would be able to S-nitrosylate cysteine thiols to make SNOs (Borodulin et al., 2014; Vanin, 2009), which are also potent vasodilators. Determination of the redox state of the NO species released by DNICs is a necessary step towards understanding their mechanism of bioactivity.

In addition to interests in the physiologic role of DNICs, their NO-mimetic properties have made them important therapeutic candidates (Vanin, 2009). Unlike other nitrodilators, glutathione-liganded BDNIC (glut-BDNIC) has long-lasting hypotensive effects and is currently in clinical trials for treatment of hypertension (Chazov et al., 2012). It has been proposed that glut-BDNIC is converted into more stable plasma albumin-liganded MDNIC in the circulation (Boese et al., 1995; Rahmanto et al., 2012; Timoshin et al., 2007). Nevertheless, the kinetics and mechanism of this conversion are not clear, let alone the effects on BDNIC-mediated vasodilation.

This study was undertaken to investigate the mechanism of glut-BDNIC-mediated

vasodilation in both isolated arteries and in vivo, and to characterize the relationship between the

hemodynamic effects and pharmacokinetics of glut-BDNIC. Using both wire myography

bioassay and chemical analysis, we test the hypothesis that DNICs release HNO rather than NO·.

Using wire myography again, we characterize the role of plasma albumin in modulating the

vasodilatory effects of glut-BDNIC. Finally, we investigate the hemodynamic effects of

glut-BDNIC and correlate this with its pharmacokinetics both in vitro and in vivo.

Materials and Methods

Experimental animals

All animal protocols were pre-approved by the Institutional Animal Care and Use Committee of

Loma Linda University, and were in accordance with guidelines of the American Physiological

Society and the National Institutes of Health.

Preparation of GSNO, DNICs, and NO gas

S-nitroso-glutathione (GSNO) and DNICs were prepared as reported previously (Borodulin

et al., 2013b; Liu et al., 2015). NO gas was generated by reaction of HCl and nitrite followed by

purification with NaOH. Further details are provided in the supplemental materials.

Surgical procedures and bolus injection protocol in sheep

Neutered male sheep nine to ten months old and weighing 37±2 kg were surgically

instrumented as previously reported (Liu et al., 2015) and described in more detail in the

supplemental materials. After surgical instrumentation, isoflurane (1.5 to 2.5%) was discontinued

and anesthesia was maintained with ketamine (1mg/kg) and vecuronium (0.1 mg/kg; Sun

Pharmaceutical, Mumbai, India) given intravenously and supplemented hourly or as needed.

L-NAME (L-N^{G}-nitro arginine methyl ester; 45 mg/kg) and hexamethonium (1 mg/kg for initial

dose; 2 mg·h^{-1}·kg^{-1} for continuous dose) were given intravenously to block endogenous NO

synthesis and sympathetic activity, respectively. After a baseline period of 30 min, a 1ml bolus

of NO$^{\bullet}$, provided by dissolving NO gas in saline, GSNO, or glut-BDNIC was injected into the

jugular vein while the mean arterial blood pressure (MAP) was recorded through a catheter in the

brachial artery. Average hypotensive responses during 120-s intervals were calculated and

normalized to the baseline values.

Surgical procedures and experimental protocol in rats

Female rats weighing 301±3 g were anesthetized and surgically prepared in a manner

similar to the sheep and as described in the supplemental materials. After surgical

instrumentation, isoflurane (2.5%) was discontinued and anesthesia was maintained with an

intraperitoneal injection of urethane (1000 mg/kg) and thereafter supplemented as required.

Hexamethonium (1 mg/kg for initial dose; 2 mg·h^{-1}·kg^{-1} for continuous dose) was given

intravenously to limit neural influences. MAP and heart rate (HR) were recorded through a

catheter in the carotid artery. Rats were given continuous infusions or bolus injections. In the

continuous infusion protocol, 25 μM glut-BDNIC or 50 μM GSNO was infused into the lower

abdominal aorta at rates of 0.05, 0.1, 0.2, and 0.4 ml/min, increasing every three minutes, doses

providing a total of ~0.19 μmol/kg glut-BDNIC or ~0.37 μmol/kg GSNO, respectively. Since

each glut-BDNIC molecule contains four NO moieties, this equates to ~0.75 μmol/kg NO moiety

during the 12-min infusion. In the bolus injection protocol, 0.29 ± 0.02 ml of 2.5 mM

glut-BDNIC (2.42 μmol/kg glut-BDNIC molecule or 9.68 μmol/kg NO moiety) was injected into

the lower abdominal aorta over five seconds. Blood samples were then collected from the jugular

vein for EPR analyses. Average hemodynamic responses during 20 –s intervals at different time

points were calculated and compared with baseline values.

Wire myography

Ovine mesenteric arterial rings (2 mm diameter and 5 mm long) were denuded of endothelium

(verified with 1 μM acetylcholine) and mounted in organ bath chambers as previously described

(Liu et al., 2016). Following preconstriction with 10 μM serotonin, dose-response curves were

measured for study drugs including glut-BDNIC, glut-MDNIC, PROLI-NONOate (NO• donor;

Cayman Chemical), GSNO, and Angeli's salt (AS; HNO donor; Cayman Chemical). Test

compounds were added to the baths five min before the contraction and maintained until the end

of the experiments. These compounds include the sGC inhibitor ODQ (1H-[1,2,4] oxadiazolo

[4,3-a] quinoxaline-1-one; 10 μM), the NO• and HNO scavenger CPTIO (2-(4-carboxyphenyl)-

4,4,5-tetramethyl imidazoline-1-oxyl-3-oxide; 200 μM), SOD (superoxide dismutase 1; 1000

U/ml), DTT (1,4-dithiothreitol; 1 mM), bovine albumin (alb; 15 μM) (all from Sigma Aldrich, St

Louis, MO), and heparinized plasma collected from sheep. Relaxation was normalized to the

tension (100%) measured just prior to the first addition of the dose-response drug. Spontaneous

changes in the tension of control vessels that did not receive a test drug were subtracted from

individual experiments before calculation of responses. Maximal absolute tensions of sheep

mesenteric arterial strips in the absence and presence of different test compounds are shown in

Supplemental Figure 2.

Hydroxylamine assay

The details are described in the supplemental materials.

Electron Paramagnetic Resonance (EPR)

EPR signals were recorded from paramagnetic DNICs at room temperature or 150 K using a

Bruker X-Band EPR spectrometer. Samples with CPTIO (50 μM) were analyzed on site at room

temperature while other samples were snap-frozen in quartz tubes (707-SQ-250M, Wilmad

LabGlass, SP Industries; PA, USA) in liquid nitrogen, and kept at -80 $^{\circ}$C until analyses. The EPR

was set to a microwave power of 20 mW and modulation amplitude of 0.1 G for room

temperature measurements, and 2 mW and 1.0 G, respectively, for measurements at 150 K. A

standard curve of glut-MDNIC (1-50 μM) was made daily. While glut-BDNIC *per se* was

EPR-silent (EPR un-measureable), the metabolite formed in the presence of plasma or albumin

had an EPR spectra similar to that of MDNICs and was quantified using the standard curve of

glut-MDNIC. The intensity of the EPR signal, an index of the amount of unpaired electrons, was

quantified by double integration using *WIN-EPR* (Bruker, Billerica, MA).

Modification of albumin

To test for interactions of glut-BDNIC with albumin, the protein was modified chemically. Albumin (840 μM) in PBS at pH=7.4 was incubated with the thiol modifier $HgCl_2$ (5 mM) and/or the histidine modifier diethylpyrocarbonate (5 mM) at room temperature for 40 min, and then desalted using a Sephadex™ G-25 column with an exclusion limit of 5000 M_r (GE Healthcare, Sweden).

Statistics

Average values are given as mean ±SEM in the text and figures. Statistical analyses were carried out with *Prism*, v5.0c (Graphpad Software, La Jolla, CA) with significance accepted at p<0.05. One-way ANOVA with Dunnett's test was used to test significance of changes associated with rates of intravenous infusion. Student's t-test was used where indicated. Relaxation results from wire myography experiments were quantified and compared by fitting the data to the Gaddum/Schild model in *Prism*. Rates of DNIC elimination from circulating blood were quantified by fitting the concentration vs time curve to a one-phase decay function using *Prism* after subtraction of baseline concentrations (nil).

Results:

Verification of laboratory-prepared DNICs

The UV-Vis spectra of glut-BDNIC and glut-MDNIC were as others have found (Borodulin et al., 2014), indicating successful synthesis (Fig. S1). glut-MDNIC displayed a typical EPR signal with an axially symmetric g-factor with $g_\perp$=2.04, $g_\parallel$=2.014, and g_{av}=2.03. glut-BDNIC, which itself is diamagnetic, was EPR silent indicating no detectable contamination with glut-MDNIC. The prepared glut-BDNIC was 99.5±0.7% pure as estimated by the extinction coefficient of $7400M^{-1}cm^{-1}$ at 360 nm (Borodulin et al., 2014).

Role of HNO in BDNIC-mediated relaxation

The relaxation of isolated ovine arterial rings induced by glut-BDNIC was eliminated by the sGC inhibitor ODQ (Fig. 1A; does not degrade DNICs, as described in the supplemental materials), indicating that the relaxation is sGC dependent (Moro et al., 1996). CPTIO, which scavenges both NO· and HNO (Goldstein et al., 2003; Samuni et al., 2010), attenuated the response to glut-BDNIC (Fig. 1A) as evidenced by a decrease in the pEC_{50} from 6.03±0.16 to 5.33±0.13 (p<0.05). In order to assess whether the attenuating effects of CPTIO on glut-BDNIC-mediated vasodilation were due to HNO or NO· scavenging, we compared the effects of CPTIO on dose response curves to known donors of either HNO (Angeli's salt; AS) or

NO· (Proli-NO). Similar to its attenuation of glut-BDNIC-mediated vasodilation, CPTIO resulted in a partial right-shift in the dose-response curve to HNO (Fig. 1D, pEC_{50} from 5.7 ± 0.2 to 5.1 ± 0.2). In contrast, vasodilatory responses to NO· were almost completely blocked (Fig. 1C, pEC_{50} from 6.0 ± 0.1 to an extent that the EC_{50} could not be calculated). Notably, the effect of CPTIO on vasodilation by glut-BDNIC was similar in magnitude to its effect on the AS dose response curve, consistent with release of HNO by glut-BDNIC.

To further test the possibility that glut-BDNIC releases HNO, the effects of CPTIO were compared in the presence and absence of SOD, which readily converts HNO into NO· (Zeller et al., 2009). In the presence of SOD, the ability of CPTIO to attenuate vasodilation by glut-BDNIC was enhanced to a level comparable to its ability to attenuate vasodilation by NO· (Fig. 1A and 1B, $p<0.05$ at log[BDNIC](M) = -5.30), consistent with the idea that SOD was converting HNO to NO· which is more efficiently scavenged by CPTIO. SOD potentiated the right-shift caused by CPTIO for both glut-BDNIC and AS, but had no effect on NO·-induced relaxation (Fig 1B, C, and D). In further support of the involvement of HNO, the HNO scavenger DTT (Zeller et al., 2009), which significantly blocked relaxation by the HNO donor AS (Fig. 1E), also blocked glut-BDNIC-mediated relaxation (Fig. 1F). Taken together, these findings demonstrate a potent vasodilatory activity of glut-BDNIC in isolated arterial rings and suggest a role for the release of HNO.

Parallel experiments were performed using glut-MDNIC. As shown in Supplemental Figure

3A, SOD alone did not alter glut-MDNIC-mediated relaxation, and CPTIO only partially

inhibited it. However, the inhibitory effects of CPTIO were potentiated by the presence of SOD.

Furthermore, glut-MDNIC-mediated vasodilation was blocked by ODQ, and significantly

attenuated by DTT (Supplemental Figure 3B). These parallel findings are all consistent with

glut-MDNIC acting as an HNO donor in a manner similar to glut-BDNIC.

Chemical Verification of glut-DNICs as HNO donor

In order to further test the hypothesis that glut-DNIC releases HNO, experiments were

conducted based on the recently reported distinction between the reactions of HNO and $NO^\bullet$ with

CPTIO (Samuni et al., 2010), which demonstrate that EPR can be used to distinguish between

the products of CPTIO reacting with either NO· or HNO. Consistent with previous reports

(Samuni et al., 2010), we found CPTIO to have a five-peak EPR spectrum (Fig. 2A). This

spectrum was rapidly converted to a seven-peak spectrum upon reaction of the CPTIO with NO·

provided by the NO donor PROLI-NONOate (Fig. 2B). In contrast, the five-peak CPTIO

spectrum gradually disappeared over a period of 90 min if the CPTIO was allowed to react with

HNO from excess AS (Fig. 2D). Finally, addition of an oxidizing solution of

$CuSO_4/H_2O_2$/ferricyanide (10μM/10mM/1mM) resulted in the seven-peak spectrum (Fig 2D).

These findings are consistent with previous work characterizing the EPR spectra of CPTIO

products of reaction with NO· or HNO, as well as oxidation of the product of the reaction of

CPTIO with HNO (Samuni et al., 2010). Importantly, similar to AS, addition of glut-BDNIC to

CPTIO resulted in a complete loss of the EPR spectrum, which could be restored to the

seven-peak spectra by the addition of $CuSO_4/H_2O_2$/ferricyanide (Fig. 2E). Notably, glutathione

(GSH) alone at comparable level did not eliminate the EPR signal of CPTIO (Fig. 2C),

indicating that the effect of glut-BDNIC on the CPTIO spectra was not due to GSH

contamination. Taken together, these results are consistent with the idea that glut-BDNIC

releases HNO, not NO·. In addition, the EPR signal of CPTIO was also eliminated by

glut-MDNIC (data not shown), suggesting the same conclusion may be applied to glut-MDNIC.

Further experiments were performed to characterize the NO species released from

glut-BDNIC. Using HEPES buffer (pH 7.4) as reagent in a purge vessel in line with a

chemiluminescence NO· analyzer, the NO· release from glut-BDNIC was compared to that from

the NO· and HNO donors. Similar to AS but different from Proli-NO, glut-BDNIC released

minimal amounts of NO·. These results were not affected by the presence of isolated mesenteric

artery tissue in the purge vessel (Supplemental Figure 4), indicating glut-BDNIC is a poor donor

of NO·. To further investigate the oxidative state of NO species released from glut-BDNIC,

measurements of hydroxylamine, one product of HNO reduction, were made following

incubation of glut-BDNIC in PBS at pH 6.8. After 5 min incubation at 95 Celsius, 20 μM

hydroxylamine was formed from an initial concentration of 250 μM glut-BDNIC. In contrast,

levels of hydroxylamine were undetectable following incubation of NO· or GSNO (for the test of

NO·+GSH) (Fig. 1G). These results are again consistent with the possibility that glut-BDNIC is a

donor of HNO rather than NO·.

Glut-BDNIC loses hypotensive effects in vivo

Contrary to the potent relaxation found in isolated arteries in the vessel baths (Fig 1),

glut-BDNIC did not reduce blood pressure when low doses were given by continuous infusion in

rats (Fig 3A). On the other hand, GSNO given at comparable doses was vasodilative both in vivo

and in vitro (Fig 3B, Fig 4E). Similar results were obtained in sheep given low doses of

glut-BDNIC or GSNO by bolus injection (Fig 4A). The hypotensive responses to bolus

injections of NO·, GSNO, and glut-BDNIC in sheep are shown in Figure 4B-D. One possible

reason for the lack of response in vivo is that that glut-BDNIC is converted in circulating blood

into a form that does not release HNO as readily. Another possibility is that any HNO that might

be released from glut-BDNIC is rapidly scavenged by reaction with other components present in

the blood but not in the vessel baths. Notably, the observation that 50 µM GSNO caused

vasodilation at 0.1 ml/min while 25 µM glut-BDNIC (which contains 100 µM NO moieties)

infused at 0.4 ml/min had no effect (Fig. 3) suggests that the production of SNOs from

glut-BDNIC in vivo, if it occurs at all, accounts for less than 1/8 of the NO moieties in

glut-BDNIC.

Role of plasma albumin in the loss of hypotensive effects of glut-BDNIC

Further tests were carried out in isolated arteries to learn what component of blood might prevent glut-BDNIC-induced vasodilation. The iron chelators PIH (pyridoxal isonicotinoyl hydrazone) and EDTA (ethylene diamine tetraacetic acid) did not affect the glut-BDNIC-mediated relaxation (Fig 5B) indicating no role for endogenous iron chelators.

Addition of heparinized plasma to the vessel bath significantly right-shifted the dose response curve of glut-BDNIC ($p < 0.05$; Figure 5A), indicating that one of its components contributes to the loss of hypotensive effects of glut-BDNIC in vivo (Fig 3A). Similar to plasma, albumin alone right-shifted the dose response curve of glut-BDNIC significantly ($p < 0.05$; Fig 5C) indicating it plays a role, perhaps by either scavenging HNO or stabilizing the BDNIC and thus inhibiting its release of HNO. The first possibility was tested and ruled out by the finding that plasma did not significantly attenuate AS-mediated relaxation (Supplemental Figure 5). To test whether the histidine or cysteine residues of albumin were involved in stabilization of glut-BDNIC, experiments were carried out with covalently modified albumin. Modification of histidine residues resulted in no change in the attenuating effects of albumin on BDNIC-mediated relaxation (Fig. 5D). Modification of the cysteine-thiols, however, resulted in a loss of the attenuating effects of albumin ($p < 0.05$; Fig 5D). These results indicate that the cysteine-thiol but not the histidine residue in albumin plays an important role in attenuating the vasodilatory effects of glut-BDNICs. Whole blood contracted the isolated arterial rings

significantly and thus its effects on glut-BDNIC-mediated relaxation were not tested.

Parallel experiments were performed to evaluate the effects of plasma and albumin on

vasodilation by glut-MDNIC. In contrast to the significant attenuating effects of plasma and

albumin on glut-BDNIC-mediated vasodilation, neither plasma nor albumin significantly altered

glut-MDNIC-induced relaxation (Supplemental Figure 6), suggesting the functional effects of

glut-BDNIC differ from those of glut-MDNIC under these conditions..

Long-lasting hypotensive effects and pharmacokinetics of BDNIC

Differing from low doses, high doses of glut-BDNIC led to long-lasting hypotensive effects

in intact rats (Fig 6A). Within 3 min after infusion of the EPR-silent glut-BDNIC, an

MDNIC-like EPR signal was detected in blood samples, although a shallow shoulder appeared

on the left side of the spectrum (Fig 6C). A similar spectrum with shallow shoulder could be

observed after addition of glut-BDNIC to isolated blood, plasma, and albumin solutions

(Supplemental Figure 7). These findings suggest that glut-BDNIC is rapidly converted to an

MDNIC-like species whether infused in vivo or added to blood, plasma, or albumin solutions in

vitro. Glut-BDNIC retained some vasodilatory activity in vivo, albeit at markedly higher doses.

The intensity of the EPR signal at the first time point (3 min) following infusion of

glut-BDNIC corresponded to 70.9 ± 2.9 μM MDNIC (Fig 6D). This concentration is comparable

to that which would be predicted based on a volume of distribution equal to the rat blood volume

((4.84 µmol Fe(NO)$_2$ nuclei infused per kg ÷ 0.068 liter of blood per kg = 71.1µM), assuming a

blood volume in rats of ~0.068 l/kg (Lee and Blaufox, 1985), suggesting that all glut-BDNIC

administered were converted to MDNIC-like metabolites that were retained in the blood. The

time course of the DNIC disappearance from the circulation followed first-order reaction kinetics

with a half-life of ~44 minutes (Fig 6D). Thus, the long duration of the hypotensive effects may

be at least partially attributed to the relatively long elimination half-life of the MDNIC-like

metabolite.

Conversion and distribution of BDNIC in blood in vitro

Given the evidence that intravenously administered glut-BDNIC is rapidly and completely

converted into MDNIC-like metabolite in vivo, we sought to characterize the conversion and

distribution of glut-BDNIC in blood in vitro. Addition of EPR-silent glut-BDNIC to either lysed

red blood cells (RBCs) or plasma both resulted in an EPR-detectable MDNIC-like metabolite

efficiently. In contrast, glut-BDNIC added to the low molecular weight (LMW) fraction of

plasma remained EPR-silent (Fig 7A). Compared to native plasma, the conversion of

glut-BDNIC into EPR-detectable species was about 50% less efficient in the presence of only the

high molecular weight (HMW) fraction of plasma or albumin solution (Fig 7A). Thus the HMW

fraction of plasma and the albumin therein play important roles in converting glut-BDNIC to

MDNIC-like metabolites, and this conversion may be facilitated by one or more components

found in the LMW fraction of plasma.

Similar to plasma and lysed RBCs, whole blood converted glut-BDNIC into MDNIC-like

metabolite (Fig 7B). All of the EPR-detectable metabolite was recovered in the plasma

compartment of whole blood, indicating that the conversion to MDNIC-like metabolite occurs in

the plasma and not in the interior of RBCs. In comparison with whole blood, washed RBCs

suspended in saline were less effective at converting glut-BDNIC (Fig 7B) into an

EPR-detectable species, in agreement with the conclusion that plasma and probably the albumin

therein play important roles in the conversion. No MDNIC-like metabolite was detected in the

RBCs of plasma-free blood indicating that glut-BDNIC itself, without binding to plasma proteins,

was also not membrane permeable.

Following addition of glut-BDNIC to whole blood, most of the MDNIC-like metabolite was

recovered in the HMW fraction of plasma, consistent with its binding to plasma proteins (Fig

7C). In addition, after adding glut-BDNIC to blood, plasma, or dissolved albumin, the EPR

spectra obtained at room temperature did not display an isotropic hyperfine structure (seen as

multiple sharp peaks pointing upward at the left side of the spectrum vs down on the right side in

the bottom spectrum of Supplemental Figure 8) that is characteristic of LMW but not HMW

MDNIC (Vanin, 2009).. These results further support the conclusion that the glut-BDNIC in

blood and plasma were converted to HMW complexes likely containing albumin.

Discussion

The results of the present experiments are consistent with previous work demonstrating that glut-BDNIC is a potent vasodilator via sGC activation (Vanin, 2009). However, contrary to previous propositions that DNICs are donors of NO· and NO^+ (Borodulin et al., 2013a; Vanin, 2009), we present both functional and chemical evidence that glut-DNIC acts by releasing HNO. In addition, our results suggest that the vasodilating potency of glut-BDNIC is markedly attenuated in the presence of plasma proteins (such as albumin), likely through an interaction with the cysteine residues.

What is the redox state of the NO moieties in DNIC?

The redox state of NO moieties in DNICs has been uncertain. Based on x-ray studies, the $Fe(NO)_2$ core has been formulated as either $Fe^{II}(NO^•)(NO^-)\}^9$ or $\{Fe^{III}(NO^-)_2\}^9$, in which the NO moieties have partial negative charges (Tsai et al., 2015; Tseng et al., 2015) and thus might be expected to be released in the form of HNO. Alternatively, others have proposed the core to exist as $\{Fe^I(NO^+)_2\}^7$, representing the NO moieties as positively charged (Borodulin et al., 2014; Borodulin et al., 2013a; Vanin, 2009). The latter formulation is supported by evidence that DNICs can S-nitrosylate thiols to produce SNOs (Boese et al., 1995; Bosworth et al., 2009; Stojanovic et al., 2004; Vanin, 2009; Vanin and Burbaev, 2011).

The current results support the idea that DNICs are donors of HNO rather than NO· or NO^+. There are multiple reasons to put forward this conclusion. First, we find that the attenuation

effects of CPTIO on glut-BDNIC-mediated vasodilation are comparable to its effects on dilation

by the HNO donor AS. In addition, CPTIO inhibits vasodilation by the NO· donor

PROLI-NONOate more efficiently than by either glut-BDNIC or AS, suggesting that

glut-BDNIC release an NO species more like HNO than NO·. The addition of SOD, which

converts HNO to NO· (Flores-Santana et al., 2011; Zeller et al., 2009b), resulted in a marked

increase in the ability of CPTIO to attenuate glut-DNIC-mediated vasodilation, a phenomenon

that was also observed for the HNO donor AS but not for NO· itself. Likewise, vasodilation by

both BDNIC and the HNO donor AS were similarly attenuated by the addition of DTT, which

scavenges HNO by converting it to H_2NOH (Zeller et al., 2009b). These results are all more

supportive of a role for HNO than NO· in BDNIC-mediated relaxation. Furthermore, based on

the EPR-characterized distinction between the products of HNO and NO· reactions with CPTIO

(Samuni et al., 2010), we chemically confirmed glut-DNIC as an HNO donor. Besides, little NO·

was released from glut-BDNIC, whereas, hydroxylamine, a HNO metabolite was detected in

glut-BDNIC, again suggesting that glut-BDNIC is a donor of HNO rather than NO·. Like

glut-BDNIC, the similar results (Supplemental Figure 3) from our experiments with

glut-MDNIC indicate that glut-MDNIC is also a donor of HNO.

The potential sources and roles of endogenous HNO have been the subject of debate for

several decades (Switzer et al., 2009). As the most abundant cellular NO adduct (Hickok et al.,

2011), DNICs have been proposed to be the "working form" of endogenous NO activity (Vanin,

2016). Our evidence that DNICs can behave as HNO donors provides a potential mechanism of

endogenous HNO formation and implies an important role for endogenous HNO.

In addition to evidence that DNICs release HNO, several experiments reported here speak

against previous proposals that DNICs release NO^+, which then might act as an S-nitrosylating

agent (Boese et al., 1995; Bosworth et al., 2009; Stojanovic et al., 2004; Vanin, 2009; Vanin and

Burbaev, 2011). First, in contrast to the potent hypotensive effects of GSNO in rats and sheep,

blood pressure was unaffected by administration of comparable doses of glut-BDNIC (Fig 3 and

4). Such an observation suggests that little SNO was formed in vivo following glut-BDNIC

infusion (calculated above as < 1/8 of BDNIC infused). Further, EPR results demonstrated nearly

complete recovery of both B- and M- glut-DNICs as DNICs after their reaction with plasma,

excluding the possibility they were converted to SNOs (Fig 7C). There are several possible

explanations for the discrepancy between previous reports suggesting DNICs are converted to

SNOs (Boese et al., 1995; Bosworth et al., 2009; Stojanovic et al., 2004; Vanin, 2009; Vanin and

Burbaev, 2011) and the lack of evidence in our current work. First, some previous experiments

were performed using NO· as the initiator of reactions in the presence of iron and thiols

(Bosworth et al., 2009; Stojanovic et al., 2004). In these experiments DNICs were simply an

intermediate product, whereas pre-synthesized DNICs were used for the current experiments.

Therefore, in the previous studies, the SNOs might have been a byproduct of oxidation reactions

of the NO· that was used for synthesizing the DNICs. Others have reported the production of

SNOs from cellular DNICs under hypoxic or anoxic conditions, thus minimizing the possibility

of NO· oxidation reactions. However, these previous studies used $HgCl_2$ to selectively detect

SNO concentrations, a method recently found to artifactually detect DNICs as SNOs (Keszler et

al., 2017). While recent closer examinations (Hickok et al., 2011; Hickok et al., 2012) of this

issue agree with our results that production of SNOs from DNICs is not a predominant mode of

action of DNICs, if it occurs at all, we would submit that a validated method that selectively

detects SNOs in the presence of DNICs is needed in order to address this question rigorously.

What are the hypotensive effects of BDNIC and the underlying mechanisms?

The hypotensive effects of glut-BDNIC have been described by Vanin and co-workers

(Borodulin et al., 2013b; capital Te et al., 2015; Chazov et al., 2012; Lakomkin et al., 2007),

leading to the ongoing clinical development of glut-BDNIC for treating hypertension (Chazov et

al., 2012). Our results confirm these previous reports by demonstrating a prolonged hypotensive

response to high-dose bolus injection (Fig 6). In the present experiments the hypotension lasted

even longer than comparable doses used in previous reports (Borodulin et al., 2013b; Chazov et

al., 2012), perhaps due to sympathetic blockade in our animal model.

Although GSNO and glut-DNICs had similar vasodilatory potencies in isolated arterial

rings (Fig 1, S3, and 4E), their potencies differed markedly in vivo. As calculated in the results

section, GSNO was found to be at least an 8-fold more potent vasodilator than glut-BDNIC in

vivo. Notably, glut-BDNIC-induced hypotension lasted for more than 4 hours (Fig 6). Such

persistence could be at least partly attributed to the long elimination half-life of the MDNIC-like

metabolite derived from glut-BDNIC (Fig 6D), and is likely influenced by its interaction with

plasma albumin as discussed below.

How might plasma alter the vasoactivity of glut-BDNIC?

It has long been proposed that proteins stabilize DNICs (Rahmanto et al., 2012; Vanin,

2009), possibly attenuating their physiologic activity. Consistent with such stabilization we

found that plasma attenuated glut-BDNIC-mediated vasodilation both in vitro and in vivo.

Earlier other investigators have found that MDNIC could exchange its LMW thiolate ligands for

either the cysteine-thiol or histidine residues in albumin to form HMW MDNICs (Boese et al.,

1995; Timoshin et al., 2007). The present glut-BDNIC experiments support only the involvement

of the cysteine-thiol residues, however, (Fig 5D), as the vasoactivity of glut-BDNIC in the

presence of albumin was only attenuated by covalent modification of cysteine-thiol residues and

not by modification of histidine residues. This finding suggests that glut-BDNIC indeed binds to

albumin, possibly via its cysteine-thiol.

Notably, glut-BDNIC and glut-MDNIC added into plasma were both converted into HMW

metabolites (Fig 7C). The EPR spectrum of the HMW metabolite of glut-MDNIC is

indistinguishable from that of glut-MDNIC itself. In contrast, although the glut-BDNIC changes

from an EPR-silent signal to one that is similar to that of MDNICs, distinct differences in the

spectra were noted (Supplemental Figure 7). These differences may indicate that the HMW

metabolites of glut-BDNIC are not physically equivalent to the HMW metabolites of

glut-MDNIC. Consistent with this view, the significant attenuating effects of plasma and

albumin on glut-BDNIC-mediated vasodilation were not observed for glut-MDNIC-induced

relaxation (Supplemental Figure 6). These results suggest that the HMW metabolite of

glut-BDNIC is also functionally different from the HMW metabolite of glut-MDNIC. Thus,

although glut-BDNIC and glut-MDNIC display similar vasodilatory and HNO-releasing

characteristics in vitro, key differences exist between the physical characteristics and

vasodilatory effects of their HMW products in plasma, suggesting that further characterization of

the structure of the HMW glut-BDNIC metabolite is needed before concluding that it is simply a

HMW MDNIC.

The reason for the decrease in vasodilatory potency of glut-BDNIC upon reacting with

albumin is not well understood. One possibility is that the NO moieties in the $Fe(NO)_2$ core are

stabilized when the DNIC is bound to albumin. The decreased vasoactivity would then be a

result of a decreased rate of release of HNO from the HMW DNIC. Alternatively, the

albumin-bound DNIC may not release HNO, but is instead in equilibrium with a minor fraction

of LMW DNIC (Fig 7C), which is less stable (capital Te et al., 2015) and thus more likely to

release HNO. In either case, the stabilization would prolong the hypotensive effects of DNICs

and account for the relatively long biologic half-life of 44 min.

Because neither glut-BDNIC nor its HMW metabolites are membrane permeable (Figs 7B,

6D) vasodilation is not likely to involve direct interaction between DNICs and sGC. Instead, it

may result from the release of HNO from the DNIC outside the cell, which can then diffuse into

the smooth muscle cells and activate the sGC either directly (Miller et al., 2009) or after

conversion to NO· (Zeller et al., 2009b). In any event the current experiments do not exclude the

possible involvement of an undiscovered vascular smooth muscle membrane transporter or

receptor-mediated dilatory signaling pathway that could be stimulated by DNICs. A further

possibility is that the hypotensive effects of glut-DNIC result from the calcitonin gene-related

peptide which can be induced by HNO via sGC activation (Favaloro and Kemp-Harper, 2007).

Some limitations of the present study should be acknowledged. First, although multiple

lines of evidence from both functional and chemical tests support glut-BDNIC as an HNO donor,

further investigation with scavengers or probes that can react selectively with HNO over NO· is

necessary. Although not currently commercially available, such compounds are under active

development and validation(Tan et al., 2015; Zhou et al., 2017). Second, depending upon the

conditions around, the redox state of NO moieties in glut-BDNIC might vary. Thus, we cannot

exclude the possibility that DNICs might exhibit distinct biochemical properties under different

environment.

Conclusion

In sum, results of this study indicate that glut-BDNIC is an HNO donor and a poor, if at all,

$NO^{\bullet}$ or NO^{+} (SNO) generator. Plasma proteins (such as albumin), via reactions involving its

cysteine-thiol residues, modulate glut-BDNIC-mediated vasodilation in such a way that

attenuates its hypotensive potency but prolongs its duration of action.

Acknowledgements

Disclosures

None.

Author Contributions

Research Design: Taiming Liu, Meijuan Zhang, Hobe Schroeder, Sean Wilson, Gordon Power,

Qian Li, Trent E. Tipple, Dan Borchardt, Arlin Blood

Conduct Experiments: Taiming Liu, Meijuan Zhang, Michael H. Terry, Hobe Schroeder, Qian Li,

Dan Borchardt

Data analysis: Taiming Liu, Meijuan Zhang, Michael H. Terry, Hobe Schroeder, Sean Wilson,

Gordon Power, Qian Li, Dan Borchardt, Arlin Blood

Writing of manuscript: Taiming Liu, Hobe Schroeder, Gordon Power, Qian Li, Arlin Blood

References:

Blum-Johnston C, Thorpe RB, Wee C, Romero M, Brunelle A, Blood Q, Wilson R, Blood AB,
Francis M, Taylor MS, Longo LD, Pearce WJ and Wilson SM (2016) Developmental
acceleration of bradykinin-dependent relaxation by prenatal chronic hypoxia
impedes normal development after birth. Am J Physiol Lung Cell Mol Physiol **310**(3):
L271-L286.

Boese M, Mordvintcev PI, Vanin AF, Busse R and Mulsch A (1995) S-nitrosation of serum
albumin by dinitrosyl-iron complex. *J Biol Chem* **270**(49): 29244-29249.

Borodulin RR, Dereven'kov Icapital A C, Burbaev D, Makarov SV, Mikoyan VD, Serezhenkov
Vcapital A C, Kubrina LN, Ivanovic-Burmazovic I and Vanin AF (2014) Redox
activities of mono- and binuclear forms of low-molecular and protein-bound
dinitrosyl iron complexes with thiol-containing ligands. *Nitric Oxide* **40**: 100-109.

Borodulin RR, Kubrina LN, Mikoyan VD, Poltorakov AP, Shvydkiy VO, Burbaev DS,
Serezhenkov VA, Yakhontova ER and Vanin AF (2013a) Dinitrosyl iron complexes
with glutathione as NO and NO+ donors. *Nitric Oxide-Biol Ch* **29**: 4-16.

Borodulin RR, Kubrina LN, Shvydkiy VO, Lakomkin VL and Vanin AF (2013b) A simple
protocol for the synthesis of dinitrosyl iron complexes with glutathione: EPR, optical,
chromatographic and biological characterization of reaction products. *Nitric Oxide*
35: 110-115.

Bosworth CA, Toledo JC, Jr., Zmijewski JW, Li Q and Lancaster JR, Jr. (2009) Dinitrosyliron

complexes and the mechanism(s) of cellular protein nitrosothiol formation from

nitric oxide. Proc Natl Acad Sci U S A **106**(12): 4671-4676.

capital Te CAAC, Lakomkin VL, capital A CAAC, Ruuge EK, Kapel'ko VI, Chazov EI and Vanin

AF (2015) The hypotensive effect of the nitric monoxide donor Oxacom at different

routs of its administration to experimental animals. Eur J Pharmacol **765**: 525-532.

Chazov EI, Rodnenkov OV, Zorin AV, Lakomkin VL, Gramovich VV, Vyborov ON, Dragnev AG,

Timoshin CA, Buryachkovskaya LI, Abramov AA, Massenko VP, Arzamastsev EV,

Kapelko VI and Vanin AF (2012) Hypotensive effect of Oxacom(R) containing a

dinitrosyl iron complex with glutathione: animal studies and clinical trials on

healthy volunteers. *Nitric Oxide* **26**(3): 148-156.

Cosby K, Partovi KS, Crawford JH, Patel RP, Reiter CD, Martyr S, Yang BK, Waclawiw MA,

Zalos G, Xu X, Huang KT, Shields H, Kim-Shapiro DB, Schechter AN, Cannon RO, 3rd

and Gladwin MT (2003) Nitrite reduction to nitric oxide by deoxyhemoglobin

vasodilates the human circulation. *Nat Med* **9**(12): 1498-1505.

Favaloro JL and Kemp-Harper BK (2007) The nitroxyl anion (HNO) is a potent dilator of rat

coronary vasculature. *Cardiovasc Res* **73**(3): 587-596.

Flores-Santana W, Salmon DJ, Donzelli S, Switzer CH, Basudhar D, Ridnour L, Cheng R,

Glynn SA, Paolocci N, Fukuto JM, Miranda KM and Wink DA (2011) The Specificity of

Nitroxyl Chemistry Is Unique Among Nitrogen Oxides in Biological Systems. *Antioxid Redox Sign* **14**(9): 1659-1674.

Goldstein S, Russo A and Samuni A (2003) Reactions of PTIO and carboxy-PTIO with *NO, *NO2, and O2-*. *J Biol Chem* **278**(51): 50949-50955.

Hickok JR, Sahni S, Shen H, Arvind A, Antoniou C, Fung LWM and Thomas DD (2011) Dinitrosyliron complexes are the most abundant nitric oxide-derived cellular adduct: biological parameters of assembly and disappearance. *Free Radical Bio Med* **51**(8): 1558-1566.

Hickok JR, Vasudevan D, Thatcher GR and Thomas DD (2012) Is S-nitrosocysteine a true surrogate for nitric oxide? *Antioxid Redox Sign* **17**(7): 962-968.

Keszler A, Diers AR, Ding Z and Hogg N (2017) Thiolate-based dinitrosyl iron complexes: Decomposition and detection and differentiation from S-nitrosothiols. *Nitric Oxide*.

Lakomkin VL, Vanin AF, Timoshin AA, Kapelko VI and Chazov EI (2007) Long-lasting hypotensive action of stable preparations of dinitrosyl-iron complexes with thiol-containing ligands in conscious normotensive and hypertensive rats. *Nitric Oxide* **16**(4): 413-418.

Lee HB and Blaufox MD (1985) Blood volume in the rat. *J Nucl Med* **26**(1): 72-76.

Liu T, Schroeder HJ, Wilson SM, Terry MH, Longo LD, Power GG and Blood AB (2016) Local and systemic vasodilatory effects of low molecular weight S-nitrosothiols. *Free*

Radical Bio Med **91**:215-223

Liu T, Schroeder HJ, Zhang M, Wilson SM, Terry MH, Longo LD, Power GG and Blood AB (2016) S-nitrosothiols dilate the mesenteric artery more potently than the femoral artery by a cGMP and L-type calcium channel-dependent mechanism. *Nitric Oxide* **58**: 20-27.

Miller TW, Cherney MM, Lee AJ, Francoleon NE, Farmer PJ, King SB, Hobbs AJ, Miranda KM, Burstyn JN and Fukuto JM (2009) The effects of nitroxyl (HNO) on soluble guanylate cyclase activity: interactions at ferrous heme and cysteine thiols. *J Biol Chem* **284**(33): 21788-21796.

Moro MA, Russel RJ, Cellek S, Lizasoain I, Su Y, Darley-Usmar VM, Radomski MW and Moncada S (1996) cGMP mediates the vascular and platelet actions of nitric oxide: confirmation using an inhibitor of the soluble guanylyl cyclase. *Proc Natl Acad Sci U S A* **93**(4): 1480-1485.

Mulsch A, Mordvintcev P, Vanin AF and Busse R (1991) The Potent Vasodilating and Guanylyl Cyclase Activating Dinitrosyl-Iron(Ii) Complex Is Stored in a Protein-Bound Form in Vascular Tissue and Is Released by Thiols. *FEBS letters* **294**(3): 252-256.

Pawloski JR, Hess DT and Stamler JS (2001) Export by red blood cells of nitric oxide bioactivity. *Nature* **409**(6820): 622-626.

Rahmanto YS, Kalinowski DS, Lane DJR, Lok HC, Richardson V and Richardson DR (2012)

Nitrogen Monoxide (NO) Storage and Transport by Dinitrosyl-Dithiol-Iron Complexes: Long-lived NO That Is Trafficked by Interacting Proteins. *J Biol Chem* **287**(10): 6960-6968.

Samuni U, Samuni Y and Goldstein S (2010) On the Distinction between Nitroxyl and Nitric Oxide Using Nitronyl Nitroxides. J Am Chem Soc **132**(24): 8428-8432.

Severina IS, Bussygina OG, Pyatakova NV, Malenkova IV and Vanin AF (2003) Activation of soluble guanylate cyclase by NO donors - S-nitrosothiols, and dinitrosyl-iron complexes with thiol-containing ligands. *Nitric Oxide-Biol Ch* **8**(3): 155-163.

Shoman ME and Aly OM (2016) Nitroxyl (HNO): A Reduced Form of Nitric Oxide with Distinct Chemical, Pharmacological, and Therapeutic Properties. *Oxid Med Cell Longev* **2016**: 4867124.

Stamler JS, Singel DJ and Loscalzo J (1992) Biochemistry of nitric oxide and its redox-activated forms. *Science* **258**(5090): 1898-1902.

Stojanovic S, Stanic D, Nikolic M, Spasic M and Niketic V (2004) Iron catalyzed conversion of NO into nitrosonium (NO+) and nitroxyl (HNO/NO-) species. *Nitric Oxide-Biol Ch* **11**(3): 256-262.

Switzer CH, Flores-Santana W, Mancardi D, Donzelli S, Basudhar D, Ridnour LA, Miranda KM, Fukuto JM, Paolocci N and Wink DA (2009) The emergence of nitroxyl (HNO) as a pharmacological agent. *Bba-Bioenergetics* **1787**(7): 835-840.

Tan Y, Liu RC, Zhang HT, Peltier R, Lam YW, Zhu Q, Hu Y and Sun HY (2015) Design and

Synthesis of Near-infrared Fluorescent Probes for Imaging of Biological Nitroxyl. *Sci*

Rep-Uk **5**.

Timoshin AA, Vanin AF, Orlova TR, Sanina NA, Ruuge EK, Aldoshin SM and Chazov EI (2007)

Protein-bound dinitrosyl-iron complexes appearing in blood of rabbit added with a

low-molecular dinitrosyl-iron complex: EPR studies. *Nitric Oxide* **16**(2): 286-293.

Tsai ML, Tsou CC and Liaw WF (2015) Dinitrosyl iron complexes (DNICs): from biomimetic

synthesis and spectroscopic characterization toward unveiling the biological and

catalytic roles of DNICs. *Acc Chem Res* **48**(4): 1184-1193.

Tseng YT, Chen CH, Lin JY, Li BH, Lu YH, Lin CH, Chen HT, Weng TC, Sokaras D, Chen HY, Soo

YL and Lu TT (2015) To Transfer or Not to Transfer? Development of a Dinitrosyl

Iron Complex as a Nitroxyl Donor for the Nitroxylation of an Fe-III-Porphyrin Center.

Chem-Eur J **21**(49): 17570-17573.

Vanin AF (2009) Dinitrosyl iron complexes with thiolate ligands: physico-chemistry,

biochemistry and physiology. *Nitric Oxide* **21**(1): 1-13.

Vanin AF (2016) Dinitrosyl iron complexes with thiol-containing ligands as a "working

form" of endogenous nitric oxide. *Nitric Oxide-Biol Ch* **54**: 15-29.

Vanin AF and Burbaev D (2011) Electronic and spatial structures of water-soluble

dinitrosyl iron complexes with thiol-containing ligands underlying their ability to

act as nitric oxide and nitrosonium ion donors. *J Biophys* **2011**: 878236.

Vanin AF, Mokh VP, Serezhenkov VA and Chazov EI (2007) Vasorelaxing activity of stable powder preparations of dinitrosyl iron complexes with cysteine or glutathione ligands. *Nitric Oxide* **16**(3): 322-330.

Vanin AF, Stukan RA and Manukhina EB (1996) Physical properties of dinitrosyl iron complexes with thiol-containing ligands in relation with their vasodilator activity. *Bba-Protein Struct M* **1295**(1): 5-12.

Zeller A, Wenzl MV, Beretta M, Stessel H, Russwurm M, Koesling D, Schmidt K and Mayer B (2009) Mechanisms Underlying Activation of Soluble Guanylate Cyclase by the Nitroxyl Donor Angeli's Salt. *Mol Pharmacol* **76**(5): 1115-1122.

Zhou YB, Zhang XF, Yang S, Li Y, Qing ZH, Zheng J, Li JS and Yang RH (2017) Ratiometric Visualization of NO/H2S Cross-Talk in Living Cells and Tissues Using a Nitroxyl-Responsive Two-Photon Fluorescence Probe. *Anal Chem* **89**(8): 4587-4594.

Financial Support:

Figure Legends:

Figure 1. *Role of HNO in BDNIC-mediated relaxation in isolated sheep mesenteric arteries* ($n\geq5$ for A-F; n=3 for G). glut-BDNIC-mediated relaxation in the absence and presence of **A)** the sGC inhibitor ODQ (10 μM) or the NO· and HNO scavenger CPTIO (200μM), or **B)** the enzyme SOD (1000U/ml, converts HNO into NO$^{\bullet}$) or SOD (1000U/ml) and CPTIO (200μM). Effects of SOD (1000U/ml), CPTIO (200μM), or SOD (1000U/ml) and CPTIO (200μM) on **C)** NO$^{\bullet}$- (from PROLI-NONOate) and **D)** HNO- (from AS) mediated relaxation. The effects of DTT (1mM, HNO scavenger) on **E)** AS- and **F)** glut-BDNIC-mediated relaxation. The vessel strips were ~2 mm in diameter and 5 mm long. Information concerning the various reactions is shown in each panel. Relaxation was normalized to the tension (100%) prior to the first addition of the dose-response drug. **G)** In vitro measurements to detect the production of hydroxylamine, a metabolite of HNO, from glut-BDNIC.

Figure 2. Confirmation of glut-BDNIC as an HNO donor by EPR, utilizing the difference between HNO and NO$^{\bullet}$ reactions with CPTIO. EPR spectra of (**A**) 50 μM CPTIO alone, (**B**) 50 μM CPTIO + 200 μM NO$^{\bullet}$, (**C**) 50 μM CPTIO + 100 μM GSH, (**D**) 50 μM CPTIO + 200 μM AS, and (**E**) 50 μM CPTIO + 50 μM glut-BDNIC at different time points as indicated above in each spectrum. Spectrum for (**A**) was stable for at least three hours. Spectra shown below for (**D**)

and (**E**) were obtained after oxidation with $CuSO_4/H_2O_2$/ferricyanide (indicated as "+Fe^{3+}"). A

representative spectrum from at least three individual experiments is shown. All experiments

were performed in HEPES buffer (pH=7.4). All spectra were recorded at room temperature and

are shown in the same scale as that in (**A**).

Figure 3. Effects of glut-BDNIC (**A**) and GSNO (**B**) on mean arterial blood pressure (MAP)

and heart rate (HR) in anesthetized rats during continuous, stepped intravascular infusions ($n{\geq}5$).

Twenty-five µM glut-BDNIC, equivalent to 100 µM NO moieties, or 50 µM GSNO, equivalent

to 50 µM NO moieties, was infused at increasing rates with each rate maintained for three min.

*p<0.05, **p<0.01 vs. baseline (100%); One-way ANOVA with Dunnett's post hoc test.

Figure 4. Hypotension induced by bolus injections of NO·, GSNO, and glut-BDNIC in

anesthetized sheep. **A)** Effects of NO·, GSNO, and glut-BDNIC on mean arterial blood pressure

(MAP) following a 1.0 mL bolus given in the jugular vein ($n{\geq}4$). **B-D)** Representative

hypotensive effects of bolus injection of **B)** NO (1 ml of 2.0 mM or 54 nmol/kg), **C)** GSNO (1

ml of 2 mM or 54 nmol/kg); and **D)** glut-BDNIC (1 ml of 2.5 mM or 270 nmol/kg). **E)**

Relaxation in isolated sheep mesenteric arteries in response to GSNO (n=5). **** p<0.0001 vs.

saline (One-way ANOVA with Dunnett's post hoc test).

Figure 5. Inhibition of glut-BDNIC-mediated relaxation by albumin in plasma ($n \geq 5$).

Effects of (**A**) plasma, (**B**) chelators PIH and EDTA, (**C**) albumin (Alb), and (**D**) albumin with

modified cysteine (cys) and/or histidine (his) residuals on glut-BDNIC-mediated relaxation.

Interrupted curves in (**D**) for "control" and "intact Alb" are repeats of those in (**C**) and were

obtained in parallel with those for "modified Alb". Given that 2% v/v plasma contains ~12-16

µM albumin, 15 µM albumin was tested in (**C**) and (**D**).. Relaxation was normalized to the

tension (100%) prior to the first addition of the glut-BDNIC.

Figure 6. Long-lasting hypotensive effects of glut-BDNIC in rats after high-dose bolus

injection and pharmacokinetic findings ($n=5$). Effects of glut-BDNIC on (**A**) MAP and (**B**) HR

in rats after a bolus injection (shown as arrows at 0 min) at 2.42 µmol/kg (0.29±0.02 ml of 2.5

mM; 9.68 µmol/kg NO quantity). Note the high dose injection induces hypotensive effects

lasting several hours. **C**) EPR spectra (150 K) of blood samples collected five min before and

three min after glut-BDNIC injection, showing a comparison with those of low molecular weight

(LMW) glut-BDNIC and glut-MDNIC in PBS. Note the EPR-silent glut-BDNIC creates an

MDNIC-like detectable EPR signal in blood after administration suggesting it is converted to

MDNIC-like metabolites. **D**) Time course of disappearance of MDNIC-like metabolites in blood

in vivo. The dots are measured values, while the line is a one-phase decay curve fit to the

measured values. Values follow first order kinetics with an apparent elimination half-life of

43.6±2.0 min. *p<0.05 vs. before injection, One-way ANOVA with Dunnett's post hoc test..

Figure 7. Conversion and distribution of glut-BDNIC in blood in vitro (*n*=5). **A**) Conversion of

EPR-silent glut-BDNIC into an EPR-detectable MDNIC-like species upon addition to water,

lysed RBCs, plasma, the HMW fraction of plasma, the LMW fraction of plasma, and albumin

(600 μM) dissolved in saline. Following addition of 25 μM EPR-silent glut-BDNIC into each

component, the EPR-detectable MDNIC-like metabolite formed after 1 or 5 min of incubation

(37 C) was quantified using a standard curve of glut-MDNIC. Lysed RBCs: RBCs washed 3

times with saline then lysed by addition of water (1:1v/v) and two cycles of freeze/thaw. The

HMW and LMW fractions of plasma were separated by size-exclusion chromatography (cutoff

5000MW). Albumin was dissolved in saline at 600 μM, a concentration comparable to that of

normal plasma. The horizontal dashed line at 50μM represents the level that would be expected

if 100% of the 25 μM glut-BDNIC were converted into MDNIC. Statistical significance was

only evaluated for the 5 min incubation results (one-way ANOVA). **B**) Compartmental

distribution of the MDNIC-like metabolite formed following addition of glut-BDNIC to whole

blood (hematocrit (HCT)=33±2%) and plasma-free blood (RBCs washed 3 times with saline and

then suspended in saline (1:1 v/v); HCT=50%). Where noted, RBCs were separated from

plasma/saline by centrifugation. Statistical significance was only evaluated for the 5 min

incubation results (one-way ANOVA). **C**) Molecular weight of DNICs in plasma. glut-BDNIC

or glut-MDNIC was incubated with plasma for 5 min and then the HMW and LMW fractions

were separated by size-exclusion column prior to EPR quantification. DNIC recovery was

calculated by dividing the quantity in each fraction by the total amount added. Ten μl of 2.5mM

glut-BDNIC was added into 990μl of each bio-matrix. *p<0.05, only comparisons of interests

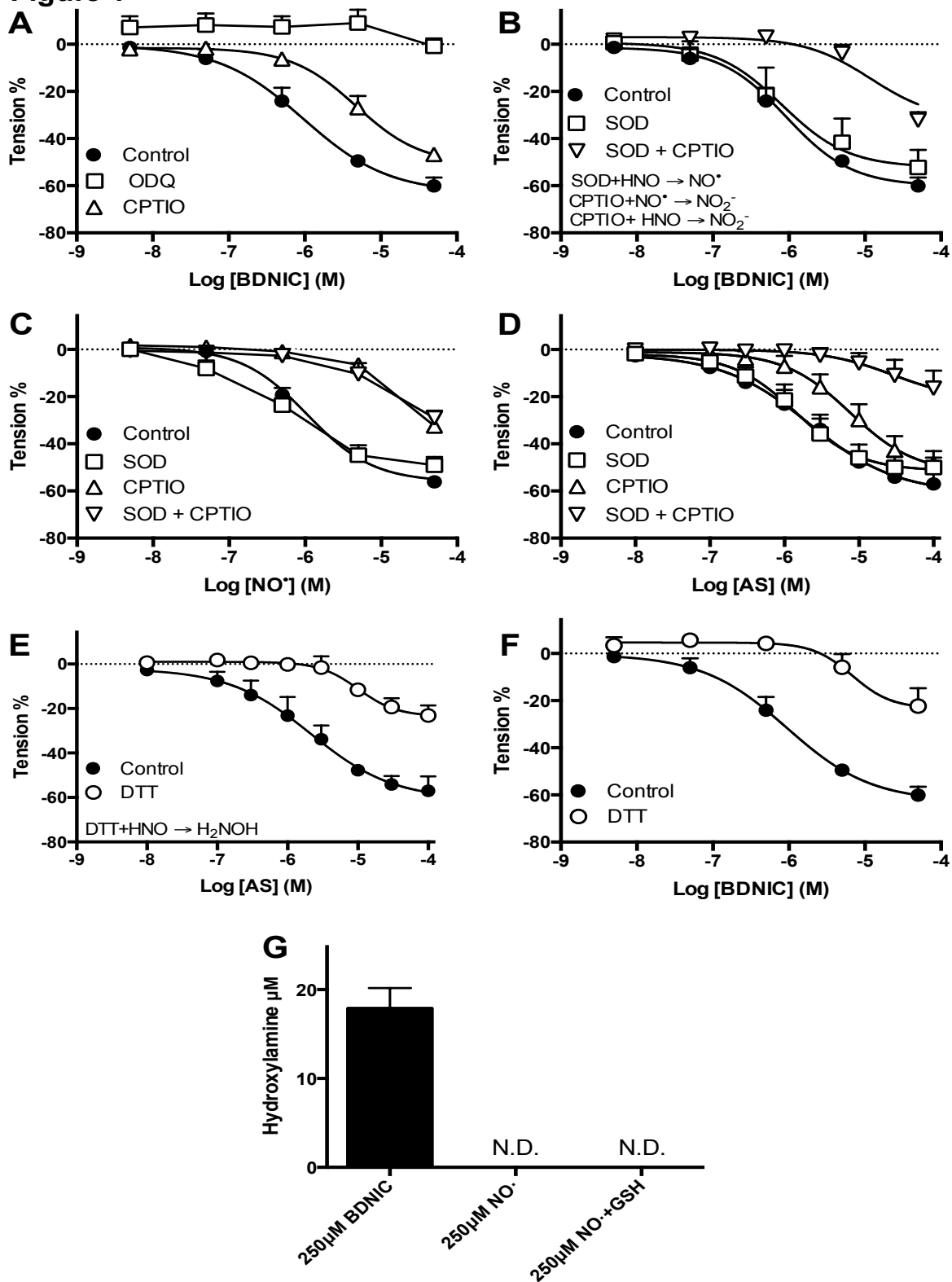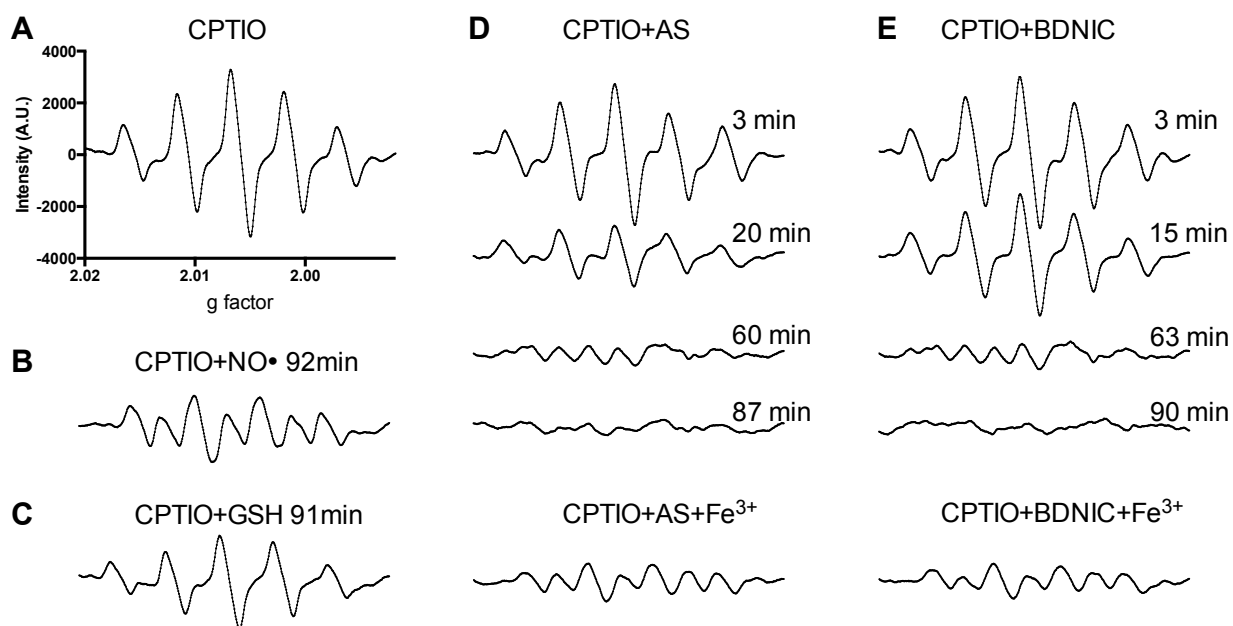were shown; N/A not applicable; N.D. not detectable.
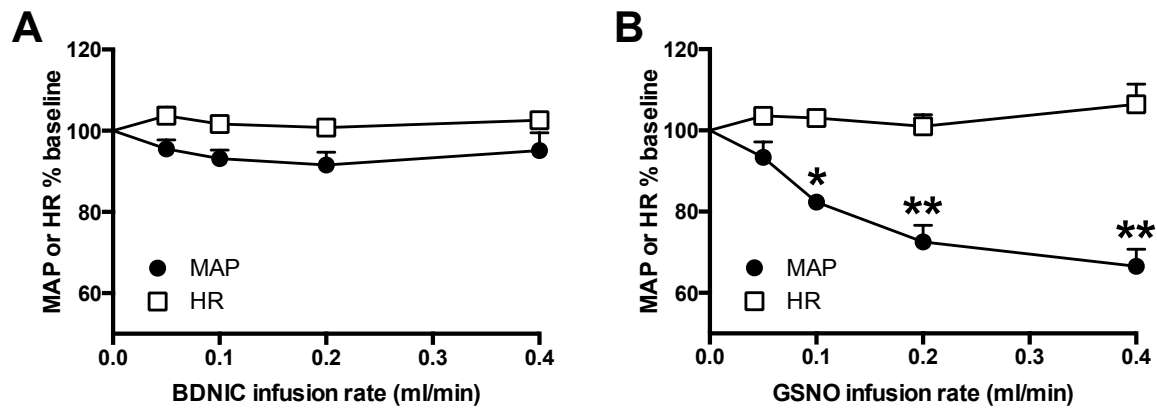
Figure 1

Figure 2

Figure 3

Figure 4
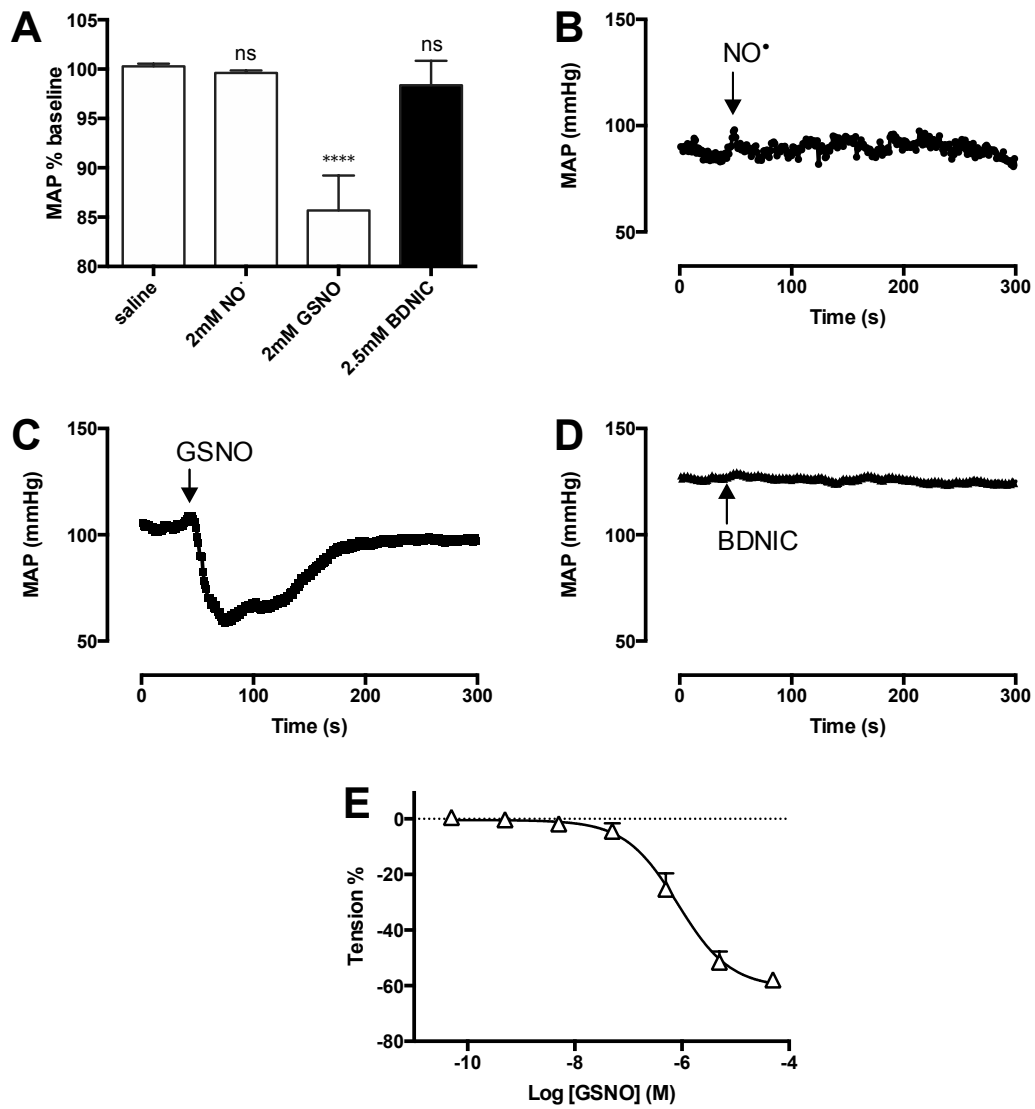
Figure 5

Figure 6

Figure 7